Temperature-Responsive Nanoparticles Enable Specific Binding of Apolipoproteins from Human Plasma

Mongkhol Prawatborisut, Jennifer Oberländer, Shuai Jiang, Robert Graf, Yuri Avlasevich, Svenja Morsbach, Daniel Crespy, Volker Mailänder, and Katharina Landfester*

Apolipoproteins are an important class of proteins because they provide a so-called stealth effect to nanoparticles. The stealth effect on nanocarriers leads to a reduced unspecific uptake into immune cells and thereby to a prolonged blood circulation time. Herein, a novel strategy to bind apolipoproteins specifically on nanoparticles by adjusting the temperature during their incubation in human plasma is presented. This specific binding, in turn, allows a control of the stealth behavior of the nanoparticles. Nanoparticles with a well-defined poly(*N*-isopropylacrylamide) shell are prepared, displaying a reversible change of hydrophobicity at a temperature around 32 °C. It is shown by label-free quantitative liquid chromatography-mass spectrometry that the nanoparticles are largely enriched with apolipoprotein J (clusterin) at 25 °C while they are enriched with apolipoprotein A1 and apolipoprotein E at 37 °C. The temperature-dependent protein binding is found to significantly influence the uptake of the nanoparticles by RAW264.7 and HeLa cells. The findings imply that the functionalization of nanoparticles with temperature-responsive materials is a suitable method for imparting stealth properties to nanocarriers for drug-delivery.

1. Introduction

Apolipoproteins are lipid binding proteins in human plasma and are mostly responsible for generating the so-called "stealth effect" around nanoparticles. The stealth effect enables a prolonged circulation time of nanoparticles in the blood after injecting nanoparticles into the body.[1] Currently, research on nanoparticles is of growing interest as they are used as drug delivery agents in nanomedicine.[2] However, the main problem when injecting nanoparticles into a bloodstream is the clearance of nanoparticles from the blood caused by an unspecific protein adsorption and fast uptake into immune cells like macrophages.[3] Therefore, controlling the protein adsorption around nanoparticles and in consequence controlling the stealth effect is of great importance.[4] Herein, we report a method for preparing a specific protein corona on nanoparticles, which significantly imparts them with a stealth effect.

The most straightforward method to provide a stealth effect to nanoparticles is to coat them with apolipoproteins prior to injection.[5] However, isolated apolipoproteins are costly, and therefore, this approach cannot be easily scaled up. Another approach relies on the enrichment of protein corona on the surface of materials with apolipoprotein by incubating functionalized nanoparticles with plasma.[6] The coating of nanocarriers with poly(ethylene glycol) (PEG) or polyphosphoesters was found to favor the adsorption of apolipoproteins.[5,7]

The protein adsorption on nanoparticles is known to be temperature-dependent.[8,9] However, no clear correlation between the composition of protein corona and the temperature could be derived.[8] Because the temperature varies in the human body, it is necessary to incubate the nanoparticles ex vivo prior to their use in vivo, in order to prepare a stable and reproducible protein corona.

M. Prawatborisut, J. Oberländer, S. Jiang, R. Graf, Y. Avlasevich,
S. Morsbach, V. Mailänder, K. Landfester
Max Planck Institute for Polymer Research
Ackermannweg 10, 55128 Mainz, Germany
E-mail: landfest@mpip-mainz.mpg.de

M. Prawatborisut, D. Crespy
Max Planck-VISTEC Partner Laboratory for Sustainable Materials
Vidyasirimedhi Institute of Science and Technology (VISTEC)
Rayong 21210, Thailand

M. Prawatborisut, D. Crespy
Department of Materials Science and Engineering
School of Molecular Science and Engineering
Vidyasirimedhi Institute of Science and Technology (VISTEC)
Rayong 21210, Thailand

J. Oberländer, V. Mailänder
Dermatology Clinic of the University Medicine of the Johannes
Gutenberg University of Mainz
Langenbeckstrasse 1, 55131 Mainz, Germany

S. Jiang
Key Laboratory of Marine Drugs
Chinese Ministry of Education
School of Medicine and Pharmacy
Ocean University of China
Qingdao 266003, China

Some reports have investigated the temperature dependence of the relationship between the protein adsorption and polymers, which undergo a transition from hydrophilic to hydrophobic properties above a lower critical solution temperature (LCST). Around two times more bovine serum albumin was adsorbed on the poly(N-isopropylacrylamide) (PNIPAM) surface at T > LCST (37 °C) compared to T < LCST (23 °C).[10] Because the LCST of PNIPAM is in the physiological range, it was used to prepare materials for biomedical applications. Thin films or beads containing PNIPAM were used for cell culture.[11] Cells spread and proliferate on the surfaces at 37 °C (T > LCST) and cell sheets could be detached and collected at T < LCST. Furthermore, beads containing PNIPAM were employed for protein separation.[11] Specific proteins in protein mixtures were adsorbed on the beads at T > LCST and eluted after lowering the temperature below LCST. PNIPAM was also used to impart a temperature-modulated release function to nanocarriers.[12] Moreover, cellular uptake of nanocarriers containing PNIPAM increased significantly at T > LCST due to favored interactions between collapsed PNIPAM chains and the cell membrane.[13]

Previously, PNIPAM-based nanoparticles with a LCST of ≈11 °C were used to isolate lysozyme, a natural antibacterial agent located in the white extract of chicken egg.[14] The nanoparticles were incubated in the extract at room temperature to catch lysozyme. Finally, apolipoproteins were found to be the major proteins detected on PNIPAM-based nanoparticles which were incubated in human plasma.[15] However, there are no reports investigating the type of preferentially adsorbed proteins on temperature-responsive nanoparticles at different temperatures and its relationship with the cell uptake.

We synthesized well-defined temperature-responsive polystyrene (PS)-PNIPAM core-shell nanoparticles with a controllable shell thickness and studied the adsorption of proteins from human plasma at various temperatures. Our hypothesis was that the incubation above or below the volume phase transition temperature (VPTT) of PNIPAM would favor a specific adsorption of certain types of apolipoproteins, which play a crucial role in imparting a stealth effect to nanocarriers. Our hypothesis was tested and verified by studying the uptake of temperature-responsive nanocarriers by RAW264.7 and HeLa cells.

2. Results and Discussion

PS-PNIPAM core-shell nanoparticles displaying a controlled PNIPAM shell thickness were prepared in order to impart the nanoparticles surface with a variable degree of hydrophilicity. Indeed, hydrophilicity has been shown to strongly affect the protein adsorption and hence, the composition and amount of protein corona.[7,16–18] The PS-PNIPAM nanoparticles were synthesized in two steps. First, core nanoparticles were synthesized by copolymerizing styrene with 5 mol% NIPAM to provide a chemical compatibility and lower the interfacial energy between the core's polymer and the outer PNIPAM shell.[19]
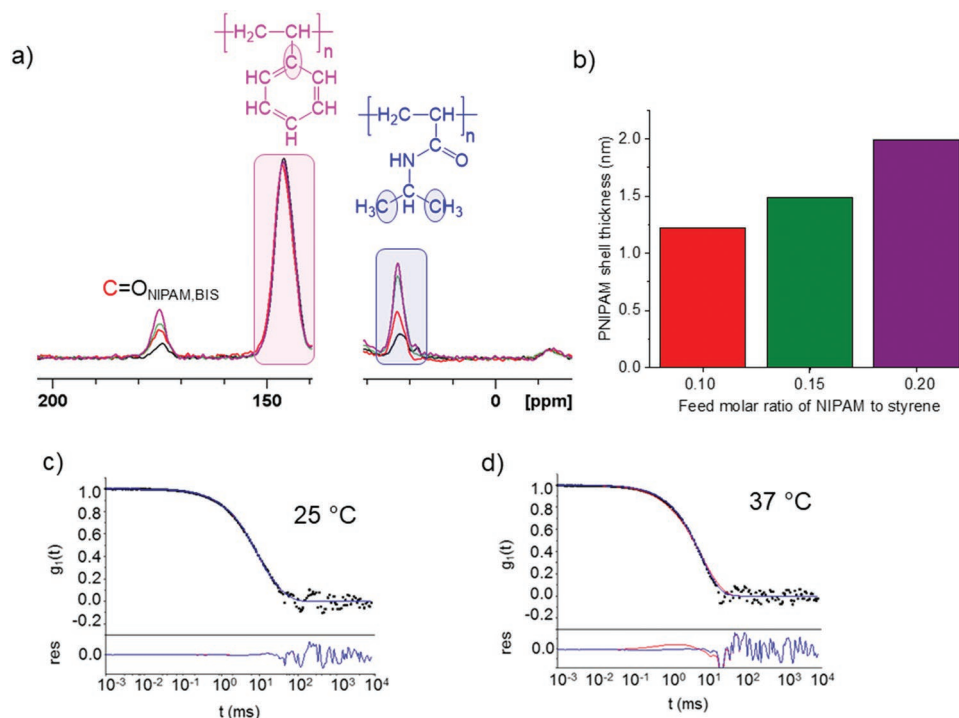

Figure 1. Characterization of the core-shell PS-PNIPAM nanoparticles with different PNIPAM shell thickness. a) Solid-state ^{13}C CP-MAS NMR spectra for determining the molar ratio of NIPAM to styrene in the nanoparticles by comparing the resonance of −CH$_3$ of NIPAM unit ($\delta = 22$ ppm) with the signals attributed to the aromatic carbon atom next to the methanetriyl unit ($\delta = 146$ ppm); PS-P0.05 (black), PS-P0.10 (red), PS-P0.15 (green), and PS-P0.20 (purple). b) Evolution of PNIPAM shell thickness against feed molar ratios of NIPAM to styrene. Intensity autocorrelation functions (ACFs) of sample PS-P0.10 in human plasma at c) 25 °C and d) 37 °C measured by multi-angle light scattering with a scattering angle of 30°. Upper graphs: ACFs of PS-P0.10 in human plasma, including data points (•), forced fit of ACFs of PS-P0.10 and proteins (red curve), and fit with additional aggregate function (blue curve). Lower graphs: Corresponding residuals resulting from the difference between data and the two fits.

Table 1. Feed molar ratios of NIPAM to styrene ($n_{NIPAM}/n_{styrene}$), molar ratios of NIPAM units to styrene units in the nanoparticles measured by solid-state ^{13}C-NMR spectroscopy ($n_{NIPAM\ units}/n_{styrene\ units}$), hydrodynamic diameter (D_h), and polydispersity index (PDI) of nanoparticles at 25 and 37 °C in water, and ζ-potential of nanoparticles at 25 °C in 1 mм KCl.

Entry	$n_{NIPAM}/n_{styrene}$ [mol]	$n_{NIPAM\ units}/n_{styrene\ units}$ [mol]	D_h (PDI) [nm]		ζ-potential [mV]
			25 °C	37 °C	
PS-P0.05	0.05	0.04	97 (0.10)	100 (0.09)	−46 ±1
PS-P0.10	0.10	0.10	102 (0.02)	102 (0.01)	−41 ± 1
PS-P0.15	0.15	0.14	98 (0.08)	99 (0.01)	−40 ± 1
PS-P0.20	0.20	0.15	104 (0.05)	103 (0.02)	−30 ± 2

The anionic surfactant sodium dodecyl sulfate (SDS) was used in the first step to stabilize the droplets of styrene in water by reducing the interfacial tension between styrene and the continuous phase of the emulsion. In a second step, the PNIPAM shell was formed around the core particle by free-radical polymerization of NIPAM with 2.6 mol% of the crosslinker *N,N'*-methylenebis(acrylamide). The amount of NIPAM in the second step was varied (Table S1, Supporting Information) to obtain core-shell nanoparticles with different PNIPAM-shell thickness.

The content of PNIPAM in the nanoparticles was quantified by solid-state ^{13}C NMR spectroscopy. The resonance of −CH$_3$ of NIPAM unit ($\delta = 22$ ppm) was compared with the signal of the aromatic carbon atom (of styrene unit) next to the methanetriyl unit at $\delta = 146$ ppm (**Figure 1**a, Figure S1, Supporting Information). The measured ratio between NIPAM and styrene units in the nanoparticles increased from 0.04 to 0.15 as their feed ratio increased from 0.05 to 0.20 (**Table 1**). The corresponding thickness of the PNIPAM shell, calculated from the amount of NIPAM units determined by ^{13}C NMR spectroscopy and the density of PNIPAM ($\rho = 1.10$ g mL^{-1}), increased from ≈1.2 to 2.0 nm (Figure 1b).[20]

Because the PNIPAM shell thickness was small, the nanoparticles did not show any significant change of average hydrodynamic diameter (D_h) upon temperature change (Table 1). Hence, the shell thickness was limited so that the average diameter of nanoparticles at various temperatures remains approximately the same, and therefore, the available surface area for protein adsorption stays constant.

Because the presence of surfactant strongly affects the protein binding on nanoparticles,[21] the nanoparticles were extensively purified. The concentration of the remaining surfactant measured by the Stains-All assay was very low (≈0.1–0.2 molecules per nm^2, Table S1, Supporting Information), so that the influence of surfactant on the protein corona is minimized.

The stability of nanoparticles in protein solutions is a prerequisite for investigating the protein adsorption. Indeed, the aggregation of nanoparticles can influence the protein adsorption profiles (e.g., amount and composition).[22] We measured the stability of PS-PNIPAM nanoparticles in human plasma by multi-angle light scattering. The VPTT of PNIPAM in solution was found to be unaffected by the presence of human serum albumin,[23] the most abundant protein in human plasma. Therefore, we assumed that the transition temperature of the PNIPAM shell would also not be altered during incubation in human plasma. The stability of nanoparticles in human plasma was evaluated based on a differential analysis of the autocorrelation functions (ACFs) obtained from

multiangle light scattering experiments performed at 25 and 37 °C (Figure 1c,d) according to the procedure described by Rausch et al.[24] First, the ACFs for pure human plasma and nanoparticles dispersion in water were determined separately. Thereafter, mixtures of nanoparticles dispersion and human plasma were evaluated with a forced fit (red line)—a sum of the individual ACFs of nanoparticles and proteins. In case that the forced fit was not sufficient to describe the measured data of the NP-protein mixture, a third aggregate term was added to the fit, shown by the blue curve. An overlapping of these two fits (blue and red curves) indicated that no aggregation occurred in the dispersion. PS-PNIPAM nanoparticles were stable in human plasma at 25 and 37 °C (Figure 1c,d, Figure S2, Supporting Information). Only for PS-P0.20, significant aggregation with aggregate sizes between 500 and 1000 nm was observed when incubated with human plasma at 37 °C. However, the size of aggregates should have no influence on cellular uptake.
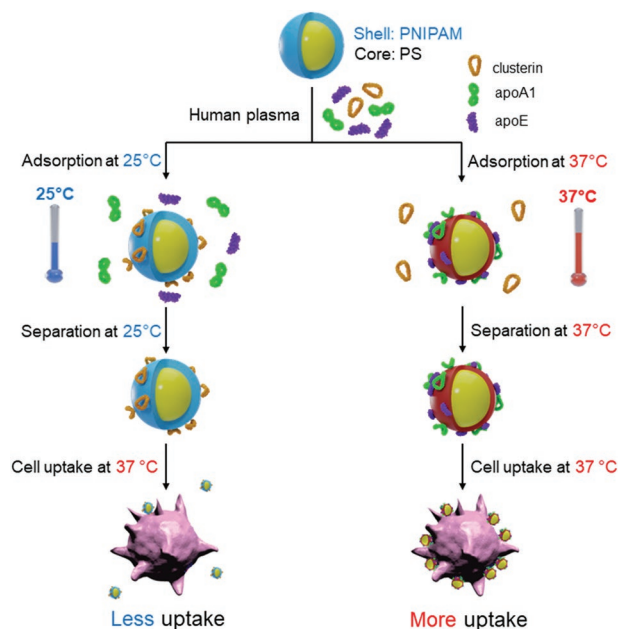

Figure 2. The catching of apolipoproteins (apolipoprotein J/clusterin, or apolipoprotein A1 and apolipoprotein E) from human plasma by temperature-responsive PS-PNIPAM nanoparticles. Apolipoprotein J is obtained in large amounts after incubating the nanoparticles in human plasma at 25 °C (T < VPTT) while apolipoprotein A1 and apolipoprotein E are adsorbed when incubating the nanoparticles in human plasma at 37 °C.

ADVANCED
SCIENCE NEWS
www.advancedsciencenews.com

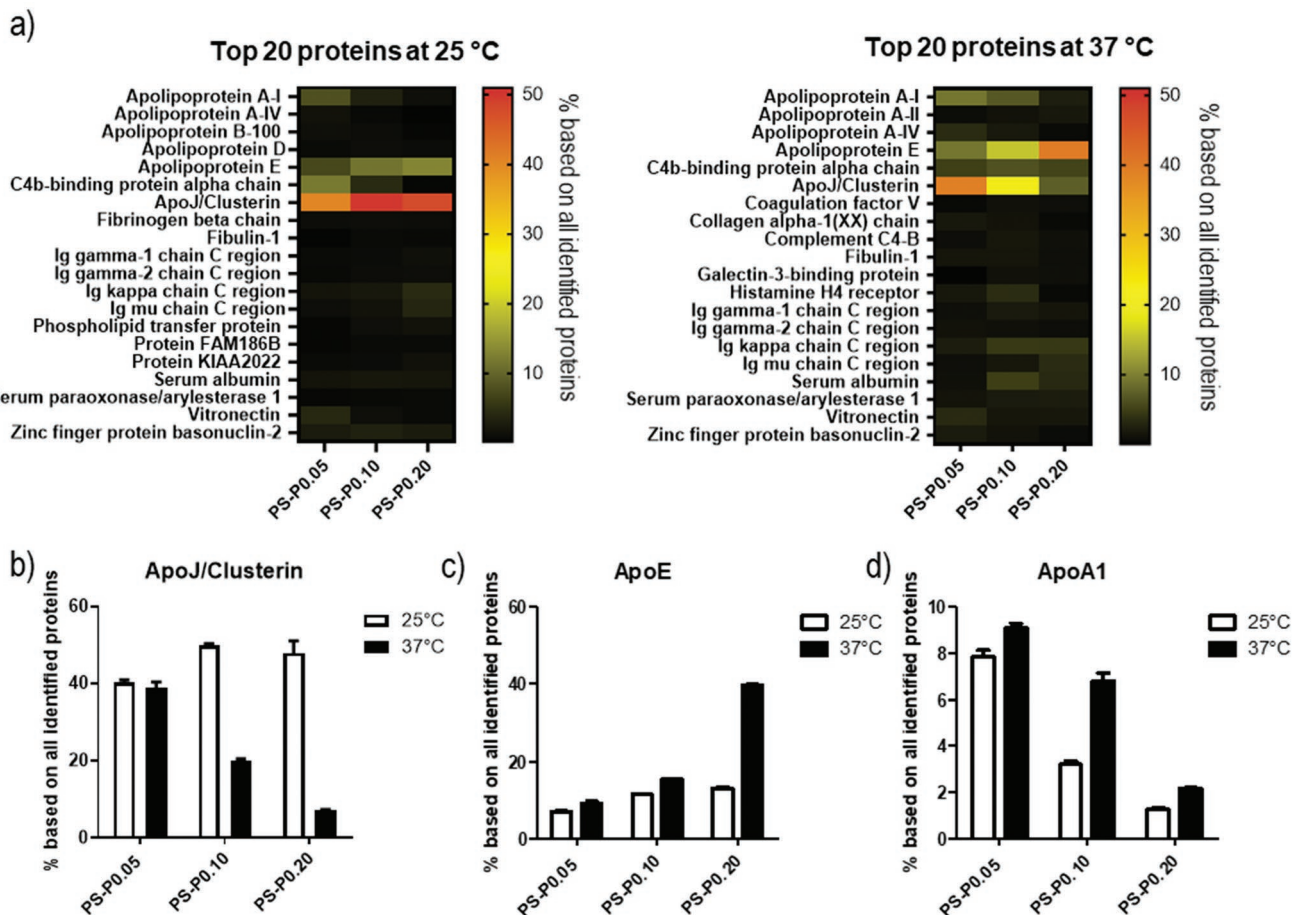NANO · MICRO
small
www.small-journal.com

Figure 3. Proteomic analysis of protein corona on the surface of PS-PNIPAM nanoparticles. a) Heatmap displaying the most abundant hard corona proteins on nanoparticles either at 25 °C or at 37 °C identified by LC-MS. b) Relative amount of Apo J (clusterin) on the surface, which is enriched on the hydrophilic surface at 25 °C. c,d) Apolipoprotein E and A1 are enriched at the hydrophobic state of nanoparticles at 37 °C. A detailed list of all identified proteins is supplemented in an excel sheet. All values are displayed as mean ± SD (n = 3).

In order to investigate the temperature-dependent formation of the protein corona, PS-PNIPAM nanoparticles were incubated in human plasma at either 25 or 37 °C for 1 h to allow the formation of a protein corona (**Figure 2**). To allow for comparable protein corona determination, the amounts of nanoparticles were fixed to 1 mg mL^{-1} plasma. Temperatures of 25 and 37 °C, the first below and the latter above VPTT, were selected to investigate the influence of hydrophobicity of PS-PNIPAM nanoparticles on protein adsorption. Moreover, protein denaturation does not occur at these temperatures. Proteins were quantified by the Pierce assay before being analyzed by liquid chromatography mass spectrometry (LC-MS). The incubation of nanoparticles at 37 °C resulted in an increased amount of total adsorbed protein in comparison to the incubation at 25 °C (Figure S3, Supporting Information). Protein adsorption is known to increase with increasing surface hydrophobicity.[17,18] The reduction of the protein adsorption below the VPTT is the first indication that the temperature change and the surface hydrophilicity change provided a stealth behavior to the nanoparticles.

The most abundant hard corona proteins and the protein composition at 25 and 37 °C were determined by LC-MS

(**Figure 3**). A list of identified proteins and their relative amounts is available in a separated Excel file. At 25 °C, below the VPTT, the PS-PNIPAM nanoparticles were enriched with Apo J (≈40% of the hard protein corona). On the contrary, the surface of PS-PNIPAM nanoparticles were enriched with apolipoprotein E and apolipoprotein A1 at 37 °C (above the VPTT). In line with previous reports,[17,18] it can be shown that changing the surface hydrophilicity influences the composition of protein corona on nanocarriers. The protein corona of nanocarriers coated with a hydrophilic polymers such as PEG were enriched with Apo J and other apolipoproteins.[25] However, coating with a hydrophobic polymer led to an enrichment with fibrinogen and immunoglobulins.[7] Herein, PNIPAM has the advantage to provide different hydrophobicity while keeping the same chemical structure. The protein corona on the surface of the nanoparticles was dependent on the PNIPAM shell thickness. No temperature dependence of Apo J binding was observed for the PS-P0.05 (very low concentration of PNIPAM) whereas the difference in enrichment of Apo J on PS-P0.20 (highest concentration of PNIPAM) was more than 40% (Figure 3b). The same trend was observed for Apo E. Indeed, with an increasing PNIPAM shell thickness the difference in Apo E enrichment

at the hydrophobic state also increased, with the highest difference of ≈26% for PS-P0.20 (Figure 3c). However, a different effect in Apo A1 binding was observed (Figure 3d). Indeed, the amount of Apo A1 was the largest on the PS-P0.05 nanoparticles. With increasing PNIPAM concentration, the amount of Apo A1 in the protein corona decreased.

The reason why some proteins preferentially attach at certain temperatures remains unclear. A possible explanation is the stability of the 3D structure at different temperatures. Serum/plasma proteins tend to have hydrophilic amino acids on the outside of their structure and hydrophobic amino acids on the inside. Therefore, the probability to unfold depending on temperature should play a major role on adsorption at different temperatures. As for the proteins of interest here (ApoA1, ApoE and ApoJ/Clusterin), no experimentally determined 3D structures were available so that it is difficult to predict in which location of the protein structure such an unfolding would occur. This is clearly a challenging but crucial task to be investigated in further research.

Furthermore, we determined whether a protein corona formed at a given temperature can be altered by a second incubation at another temperature (below and above the VPTT of PNIPAM), as it may occur during cell culture incubation. The dispersions that were previously incubated at 25 °C were centrifuged at 25 °C, re-dispersed in PBS at room temperature, and

incubated in PBS at 37 °C for 24 h. Similarly, the dispersions that were previously incubated at 37 °C were centrifuged at 37 °C, re-dispersed in PBS at room temperature, and incubated in PBS at 25 °C for 24 h. The Pierce assay revealed that the trend about the difference between total concentration of adsorbed proteins at the two different temperatures was conserved even after the second incubation at another temperature. Indeed, the total protein amount bound on the nanoparticles subjected to a second incubation was larger when the nanoparticles were first incubated at 37 °C in comparison to when the nanoparticles were first incubated at 25 °C (see Figure S3, Supporting Information). After the second incubation, the amount of protein was slightly reduced compared with the amount detected after the first incubation. We attributed this slight loss to the additional purification step. After the desorption and digestion of the proteins in the protein corona, the protein composition was analyzed by liquid chromatography and mass spectrometry. As shown in Figure S4, Supporting Information, the composition of the protein corona before and after the second incubation was not significantly different. Therefore, preferential desorption of Apo A1, Apo E, and Apo J was not observed, confirming that they are tightly bound to the nanoparticles, hence conferring stealth properties even after a change of temperature of the external media.

The adsorption of apolipoproteins, especially the adsorption of Apo J, is known to induce a prolongation of blood circulation
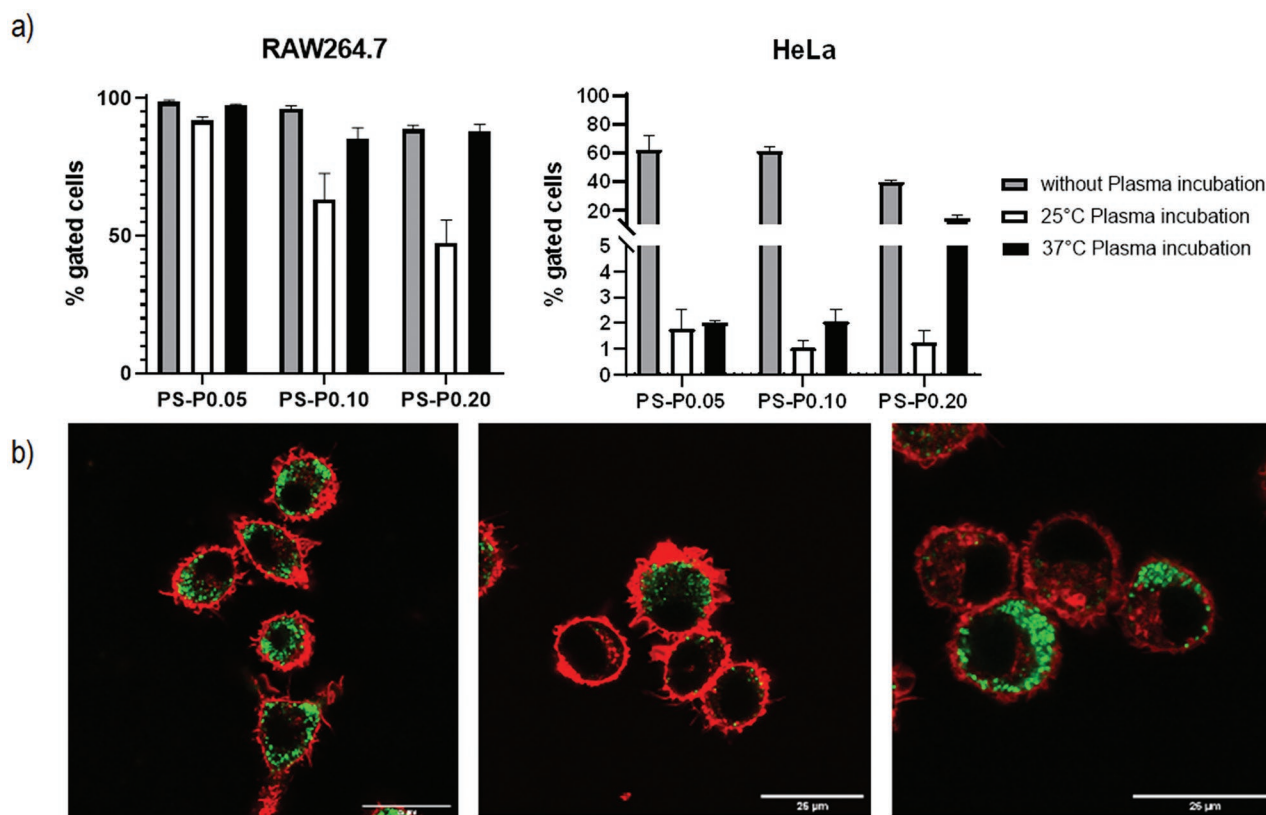

Figure 4. Cellular uptake of PS-PNIPAM nanoparticles without and after the incubation in plasma at 25 and 37 °C. a) Flow cytometry analysis of cells labelled with PS-PNIPAM nanoparticles after 4 h. Values are expressed as mean ± SD. b) Confocal laser scanning microscopy images of RAW264.7 cells incubated with PS-P0.10 nanoparticles. Left picture without plasma incubation, middle with plasma incubation at 25 °C, and right with incubation in plasma at 37 °C. The cell membrane was stained with Cellmask Deep Red and is pseudocolored in red. Nanoparticles are pseudocolored in green. Scale bars: 25 µm.

ADVANCED
SCIENCE NEWS
www.advancedsciencenews.com

NANO · MICRO
small
www.small-journal.com

time of nanoparticles and to reduce their unspecific uptake by immune cells such as macrophages.[5] Therefore, we investigated the cellular uptake of the PS-PNIPAM nanoparticles into RAW264.7 macrophages by flow cytometry and confocal laser scanning microscopy (cLSM). In order to analyze the effect of the temperature dependence on the protein corona composition, the nanoparticles were incubated at 25 or 37 °C in human plasma prior to cell uptake. Flow cytometry measurements showed a reduced uptake of nanoparticles incubated in human plasma compared with non-incubated nanoparticles, independently from the incubation temperature (**Figure 4**, Figure S5, Supporting Information). This is consistent with previous literature showing a reduced uptake of nanoparticles after their incubation with plasma or serum.[7,26] PS-P0.10 and PS-P0.20 nanoparticles incubated at 25 °C, which adsorbed the largest amount of Apo J, showed the lowest uptake into both RAW264.7 macrophages as well as into HeLa cells. For PS-P0.05 the Apo J amount in the protein corona at 25 and 37 °C was nearly the same, leading into no difference of uptake into cells. Interestingly, PS-P0.20 incubated at 37 °C showed a relatively low amount of Apo A1 and a high amount of Apo E in the protein corona. For these nanoparticles incubated at 37 °C, the difference of uptake between incubated and non-incubated nanoparticles was not as large as for the PS-P0.10 nanoparticles. This nanoparticle displayed the thickest PNIPAM shell and showed the lowest total protein amount on the surface. This shows hence that the reduced amounts of total proteins were not responsible for the stealth behavior. The stealth effect was mainly induced by specific apolipoproteins, namely Apo J (clusterin) and Apo A1. Conversely, the enrichment of the protein corona with Apo E led to an increased uptake (Figure S5a, Supporting Information).

The cLSM confirmed the internalization of the nanoparticles into the cells (Figure 4b, Figure S5c, Supporting Information). Without plasma incubation, the nanoparticles were strongly internalized. However, with Apo J and Apo A1 on their surface, the uptake was reduced. Cell viability was measured by flow cytometry using Zombie Aqua staining (Figure S5b, Supporting Information). Independently from the incubation temperature, all nanoparticles showed no toxicity on both cell lines. In addition, the high uptake of nanoparticles without plasma incubation did not show any influence on the viability of the cells.

3. Conclusions

We demonstrated that the stealth behavior of temperature-responsive nanoparticles can be controlled by adjusting the incubation temperature in human plasma, resulting in a change of composition of the protein corona. The protein corona was enriched with the stealth protein apolipoprotein J (clusterin) when incubating the nanoparticles in human plasma at 25 °C, that is, at a temperature below the VPTT of the nanoparticles. Besides, the protein corona was enriched with apolipoproteins A1 and E after incubation at 37 °C (T > VPTT). Among the prepared nanoparticles, a thickness of 1.2 nm PNIPAM was optimal for adsorbing the largest amount of Apo J at 25 °C. Furthermore, the uptake of nanoparticles after incubating in human plasma at 25 °C by RAW264.7 and HeLa cells was significantly lower than with native nanoparticles. Ultimately, we presented

a novel method to prepare stealth nanoparticles by simply incubating temperature-responsive nanoparticles in human plasma at 25 °C. It is hence a suitable method for imparting stealth properties to nanocarriers for drug delivery applications.

4. Experimental Section

Materials: 4-Hydroxybenzaldehyde (98%, Aldrich), trifluoroacetic acid (TFA, 99%, Aldrich), methacryloyl chloride (97%, Aldrich), 2,3-dichloro-5,6-dicyano-*p*-benzoquinone (DDQ, 98%, Aldrich), anhydrous dichloromethane (DCM, 99.8%, Aldrich), methanol (99.9%, Aldrich), cyclohexane (99.5%, Aldrich), petroleum ether (puriss, Aldrich), (99.8%, Aldrich), toluene (99.8%, Aldrich), 3-ethyl-2,4-dimethylpyrrole (97%, TCI Chemicals), triethylamine (99.5%, Carl Roth), *N,N*-diisopropylethylamine (DIPEA, 99.5%, Carl Roth), sodium sulfite (98%, Carl Roth), sodium sulfate (98.5%, Carl Roth), 1,8-diazabicyclo[5.4.0] undec-7-en (DBU, for synthesis, Merck), boron trifluoride etherate (for synthesis, Merck), SDS (≥ 90%, Fluka), aluminum oxide (Al$_2$O$_3$, for chromatography, Acros Organics), potassium peroxydisulfate (KPS, ≥ 99%, Merck), *N*-isopropylacrylamide (NIPAM, 98%, Acros Organics), *N,N'*-methylenebisacrylamide (BIS, 99%, Alfa Aesar), Stains-All (95%, Sigma Aldrich), isopropanol (99.96%, Fisher Scientific), and formamide (extra pure, Applichem) were used as received. Styrene (99%, Acros Organics) was purified through an aluminum oxide column prior to reaction. Unless otherwise noted, Milli-Q water was used throughout experiments.

Human blood was taken from healthy donors at the Department of Transfusion Medicine Mainz after physical examination and after obtaining written informed consent in accordance with the Declaration of Helsinki. The study was approved by the local ethics committee "Landesärztekammer Rheinland-Pfalz" (Bearbeitungsnummer: 837.439.12 (8540-F)).

Synthesis of Phenol-BODIPY (2,6-diethyl-1,3,5,7-tetramethyl-8-(4-hydroxyphenyl)-BODIPY: 4-Hydroxybenzaldehyde (244 mg, 2 mmol) and 3-ethyl-2,4-dimethylpyrrole (492 mg, 4 mmol) were dissolved in 100 mL of absolute DCM under Ar atmosphere. Three drops of TFA were added, and the solution was stirred at room temperature overnight in the dark. Dry 2,3-dichloro-5,6-dicyano-*p*-benzoquinone (DDQ) (400 mg) was added, and stirring was continued for 2 h. Triethylamine (2 mL) was added and the organic phase was washed with aqueous sodium sulfite (3%, 2 × 100 mL). Organic layers were separated, dried over anhydrous sodium sulfate, and evaporated. *N,N*-diisopropylethylamine (DIPEA) (3 mL) and 100 mL of absolute DCM were added under an Ar atmosphere, and the solution was stirred at room temperature for 10 min. BF$_3$·OEt$_2$ (3 mL) was added, and stirring was continued for 2 h. The reaction mixture was washed with an aqueous solution of NaHCO$_3$ (5%, 2 × 100 mL) and deionized water (100 mL). The combined organic extracts were dried over Na$_2$SO$_4$, filtered, and evaporated. Column chromatography with silica gel and dichloromethane as eluent afforded phenol-BODIPY which was evaporated and recrystallized from DCM/methanol to give red crystals after drying under vacuum. Yield: 642 mg (81%). ^{1}H NMR (250 MHz, CD$_2$Cl$_2$, δ): 7.15 (d, J = 8.7 Hz, 2H), 6.97 (d, J = 11.3 Hz, 2H), 5.08 (s, 1H), 2.48 (s, 6H), 2.32 (q, J = 7.5 Hz, 4H), 1.37 (s, 6H), 1.01 (t, J = 7.6 Hz, 6H); λ_{max} (toluene, ε) = 526 nm (63 000); fluorescence (toluene): λ_{max} = 542 nm (ϕ = 72%); MS (ESI) m/z [M+Na]: calcd for C$_{23}$H$_{27}$BF$_2$N$_2$NaO$_2$ 419.27; found 419.24.

Synthesis of the Polymerizable BODIPY (2,6-diethyl-1,3,5,7-tetramethyl-8-(4-methacryloyloxyphenyl)-BODIPY: Phenol-BODIPY (397 mg, 1 mmol) was dissolved in 50 mL of anhydrous dichloromethane and flushed with argon. Then DBU (305 mg, 2 mmol) was slowly added. The resulting mixture was cooled with ice-water and methacryloyl chloride (156 mg, 1.5 mmol) in dry dichloromethane (10 mL) was added dropwise. The mixture was stirred at room temperature during 24 h, and then concentrated under vacuum at room temperature. The residue purified by chromatography on silica gel (dichloromethane/petroleum ether: 70/30 vol/vol), afforded 352 mg of product (76% yield).The monomer

was dissolved in cyclohexane and freeze-dried, the resulting powder was stored in the freezer at −20 °C. ^{1}H NMR (250 MHz, CD$_2$Cl$_2$, δ):7.31 (d, $J =$ 6.2 Hz, 1H), 6.37 (s, 1H), 5.81 (s, 1H), 2.49 (s, 3H), 2.33 (q, $J =$ 7.5 Hz, 2H), 2.08 (s, 1H), 1.36 (s, 3H), 0.99 (t, $J =$ 7.5 Hz, 3H); λ_{max} (toluene, ε) = 528 nm (64 000); fluorescence (toluene): $\lambda_{max} =$ 545 nm ($\phi =$ 81%); MS (ESI) m/z [M+Na]: calcd for C$_{27}$H$_{31}$BF$_2$N$_2$NaO$_2$ 487.23; found 487.21.

Synthesis of Polystyrene-Poly(N-isopropylacrylamide) (PS-P0.05) Core Nanoparticles: Styrene (30 g, 288.05 mmol), NIPAM (1.63 g, 14.40 mmol), SDS (0.3 g, 1.04 mmol), polymerizable BODIPY (0.05 g, 0.105 mmol), and 200 mL water were charged into a 500 mL round-bottom flask. Nitrogen was bubbled through the mixture to remove oxygen for 10 min. KPS (0.3 g, 1.11 mmol) dissolved in 20 mL water was then fed into the mixture. The polymerization was performed at 80 °C for 8 h with the stirring speed of 1000 rpm. The nanoparticles were purified by dialysis to remove excessive SDS. 100 mL of the nanoparticle dispersion was placed into a dialysis tube (MWCO ≈ 14 kDa). The dialysis was performed against 10 L deionized water for 24 h while water was changed 5 times. The feed molar ratio of styrene to NIPAM was 1:0.05 and the obtained nanoparticles are denoted as PS-P0.05.

Synthesis of Core-Shell Polystyrene-Poly(N-isopropylacrylamide) Nanoparticles: To prepare PS-PNIPAM nanoparticles with varied PNIPAM shell thickness, 12.3 mL of PS-P0.05 dispersion (solid content = 10.4 wt%) was fed into a 100 mL round-bottom flask. The dispersion was diluted with 40 mL water to obtain a dispersion with a solid of 2.45 wt%. Known amounts of NIPAM and crosslinker BIS were added into the dispersions (Table S1, Supporting Information). The mixture was deoxygenized by N$_2$ bubbling for 10 min. Certain amounts of KPS were dissolved in 2 mL water, and the solution was then added to the dispersions to initiate polymerization. The polymerization was performed at 80 °C for 4.5 h with a stirring speed of 1000 rpm. Thereafter, the dispersions were dialyzed against 5 L deionized water for 24 h while changing water 5 times (MWCO ≈ 14 kDa) to remove SDS. Samples with styrene to NIPAM molar ratios of 1:0.10, 1:0.15, and 1:0.20 are denoted as PS-P0.10, PS-P0.15, and PS-P0.20, respectively. The measured residual surface concentrations of SDS in the dialyzed dispersions are shown in Table S1, Supporting Information.

Quantification of Poly(N-isopropylacrylamide) in the Core-Shell Particles by Using Solid State Nuclear Magnetic Resonance Spectroscopy: The quantitative cross polarization magic-angle spinning nuclear magnetic resonance (NMR) spectra of the nanoparticles were recorded on a 300 MHz Bruker AVANCE II spectrometer at 10 KHz MAS spinning frequency.[27] The molar ratio between NIPAM to styrene units of the particles was obtained from the NMR spectra by signal integration of the NIPAM-CH$_3$ units at 22 ppm and the quaternary aromatic site at 146 ppm, connecting the phenyl ring of PS to its aliphatic main chain. The PNIPAM shell thickness was calculated by assuming the PS and the PNIPAM formed a core and a shell in a concentric spherical structure with an external diameter equal to the hydrodynamic diameter in water determined by dynamic light scattering (DLS). The thickness of PNIPAM shell was then calculated by considering the amounts of NIPAM units determined by NMR spectroscopy for the PS-P0.10, PS-P0.15, and PS-P0.20 subtracted with the amounts of NIPAM units found in PS-P0.05, the weighted amount of styrene, the molar mass of NIPAM and styrene, and the density of both polymers which were assumed to be the density in bulk ($\rho_{PS} =$ 1.04 g mL^{-1} and $\rho_{PNIPAM} =$ 1.10 g mL^{-1}).

Stability of the Core-Shell Nanoparticles in Human Plasma: The multi-angle DLS measurements were performed on an ALV spectrometer consisting of a goniometer and an ALV-5004 multiple-tau full-digital correlator (320 channels). A He-Ne laser (wavelength of 632.8 nm) was used as a light source. For temperature-controlled measurements, the light scattering instrument was equipped with a thermostat (Julabo). Before the measurement, water, PBS, or undiluted human plasma were filtered through Millex-GS filters (Merck Millipore, Billerica, USA) with a 200 nm pore size into quartz cuvettes with an inner radius of 9 mm (Hellma, Müllheim, Germany). Prior to use, the quartz cuvettes were cleaned with acetone using a Thurmond apparatus.[28] The nanoparticles and the plasma, water, or PBS were separately incubated at 25 °C or at 37 °C before mixing (1 µL of 2 wt% NPs in 1 mL solution of plasma,

water, or PBS). Then, the mixture was incubated at 25 or 37 °C for 1 h. For data analysis, a robust multicomponent fit method reported by Rausch et al.[24] was used.

The correlation functions of nanoparticles in water and PBS at 25 and 37 °C, $g_{1,\,np}(t)$, could be fitted by a sum of two exponentials:

$$g_{1,np}(t) = a_{1,np} \text{xexp}\left(-\frac{t}{\tau_{1,np}}\right) + a_{2,np} \text{xexp}\left(-\frac{t}{\tau_{2,np}}\right) \tag{1}$$

where a_i is amplitude and $\tau_i = 1/(q^2 D_i)$ is decay time, q is the absolute value of the scattering vector ($q = 4\pi m \sin(\theta/2)/\lambda_0$) and D_i is the diffusion coefficient of particle.

Because human plasma contains many proteins and lipids with various sizes, the fit of correlation functions of pure plasma, $g_{1,p}(t)$, was more complex and hence required a sum of three exponentials:

$$g_{1,p}(t) = a_{1,p} \text{xexp}\left(-\frac{t}{\tau_{1,p}}\right) + a_{2,p} \text{xexp}\left(-\frac{t}{\tau_{2,p}}\right) + a_{3,p} \text{xexp}\left(-\frac{t}{\tau_{3,p}}\right) \tag{2}$$

When no aggregation occurred, the ACFs of nanoparticles in human plasma could be fitted by a force fit of the sum of the individual correlation functions:

$$g_{1,m}(t) = f_p g_{1,p}(t) + f_{np} g_{1,np}(t) \tag{3}$$

The variable factors in the experiments are amplitude (f_p and f_{np}). When the nanoparticles were aggregated in human plasma, the Equation (4) was extended by adding an additional aggregate term:

$$g_{1,m}(t) = f_p g_{1,p}(t) + f_{np} g_{1,np}(t) + f_{agg} g_{1,agg}(t) \tag{4}$$

where f_{agg} is the amplitude weighted by intensity of the aggregates, and the unknown correlation function of the aggregates ($g_{1,agg}(t)$) was described as:

$$g_{1,np}(t) = a_{1,agg} \text{xexp}\left(-\frac{t}{\tau_{1,agg}}\right) \tag{5}$$

Accordingly, the diffusion coefficient of the aggregates is obtained for each scattering angle (all different scattering vectors q). After extrapolation to $q = 0$, the average hydrodynamic radius of the aggregates ($R_{h,\,agg}$) was then be calculated from the Stokes-Einstein equation.

$$R_h = \frac{kT}{6\pi\eta_0 D_{q=0}} \tag{6}$$

where k is the Boltzmann's constant ($k = 1.38 \times 10^{-23}$ JK^{-1}), T is temperature, and η_0 is the kinematic viscosity of the medium.

Protein Corona Preparation: Protein corona experiments were performed as previously described from our group.[7,29,30] A constant amount of nanoparticles was chosen in order to ensure reproducibility. Therefore, 1 mg of each nanoparticle was incubated in 1 mL of human citrate plasma for 1 h either at 25 or 37 °C under constant agitation (300 rpm). Afterward, nanoparticles were centrifuged (20 000 g; 1 h; 25/37 °C) and resuspended in 1 mL PBS. For the removal of unbound and loosely bound proteins, the nanoparticles were washed 3 times with PBS. Hard corona proteins were detached from the particles using 2% (w/v) SDS and 62.5 mM Tris*HCl at 95 °C for 5 min. The protein containing supernatant was collected after centrifugation (20 000 g; 1 h; 25/37 °C) and used for protein quantification, SDS-PAGE and LC-MS analysis.

Protein Quantification: The protein concentration was determined by the Pierce 660 nm protein Assay (Thermo Scientific) according to the manufacturer's instructions. The adsorption was measured at 660 nm with a Tecan Infinite M1000 plate reader using bovine serum albumin as standard.

Sodium Dodecyl Sulfate-PAGE: The protein separation with SDS PAGE was performed using a NuPAGE 10% BisTris Gel, SeeBlue Plus2 Pre-Stained Standard (Invitrogen) as a marker, and NuPAGE MES SDS as running buffer. An absolute amount of 2 µg in 26 µL hard corona proteins were mixed with 4 µL NuPage Reducing Agent and 10 µL NuPage LDS Sample Buffer. The samples were loaded onto the gel and ran for 1.25 h at 100 V. Gels were stained with the Pierce Silver Stain Kit according to the manufacturer's manual (all materials from Thermo Fisher Scientific).

In Solution Digestion: The proteomic analysis was performed as previously described from our group.[7,29] Prior to digestion, SDS was removed from the protein solution using the Pierce Detergent Removal Spin Columns (Thermo Fisher Scientific). Afterward, the protein precipitation was performed via the ProteoExtract protein precipitation kit (CalBioChem) according to the manufacturer's manual. Proteins were isolated by centrifugation (14 000 g; 10 min) and resuspended with RapiGest SF (Waters) in ammonium bicarbonate (50 mM) buffer. The reduction of the proteins was performed using dithiothreitol (Sigma-Aldrich) (5 mM) for 45 min at 56 °C followed by alkylation with iodacetoamide (Sigma-Aldrich) (15 mM) for 1 h at rt in the dark. A protein: trypsin ratio of 50: 1 was used for tryptic digestion (18 h; 37 °C) and stopped by lowering the pH with 2 µL hydrochloric acid (Sigma-Aldrich). Degradation products of RapiGest SF were removed by centrifugation (14 000 g; 15 min; 4 °C).

Liquid Chromatography Mass Spectrometry Analysis: For absolute protein quantification, samples were diluted with 0.1% formic acid and spiked with 50 fmol µL^{-1} Hi3 *E. coli* (Waters). The peptide solution was applied to a nanoACQUITY UPLC system coupled to a Synapt G2-Si mass spectrometer. The electrospray ionization (ESI) was operated in positive mode with a NanoLockSpray source. A sample flow rate of 0.3 µL min^{-1} was used and the reference Glu-Fibrinopeptide (150 fmol µL^{-1}) at a flow rate of 0.5 µL min^{-1} was injected into the system. Synapt G2-Si was operated in resolution mode performing data-independent acquisition (MS^E) experiments. Data analysis was performed with MassLynx 4.1. Proteins were identified using Progenesis GI (2.0) and a reviewed human database downloaded from Uniprot. Noise reduction thresholds were set for low energy, high energy, and peptide intensity to 120, 25, and 750 counts. For the protein and peptide identification, the following parameters were used: Maximum protein mass 600 kDa, one missed cleavage, fixed carbamidomethyl modification for cystein, variable oxidation for methionine and false discovery rate of 4% for proteins. For the protein identification, at least two assigned peptides and five assigned fragments are required. The peptide identification needs three assigned fragments. The TOP3/Hi3 approach provided the amount of each protein in fmol.[31]

Cell Culture: RAW 264.7 cells and Human cervix carcinoma cells (HeLa) were cultured in Dulbecco's modified eagle medium (DMEM) supplemented with 10% FBS, 100 U mL^{-1} penicillin, 100 mg mL^{-1} streptomycin, and 2 mM glutamine. Cells were grown in a humidified incubator at 37 °C and 5% CO$_2$. The cell passaging and harvesting was performed using 0.25% Trypsin-EDTA for 5 min at 37 °C, 5% CO$_2$ (all reagents from Thermo Fisher Scientific). The cell viability and count were determined by using trypan blue and measuring by an automated cell counter (TC10, Bio-Rad, Germany).

Flow Cytometry: The nanoparticle uptake and cytotoxicity experiments were performed by flow cytometry. Therefore, HeLa and RAW 264.7 cells were seeded at a density of 150 000 cells per well in 24 well plates (Greiner) and incubated over night at 37 °C and 5% CO$_2$. Prior to the uptake experiment, DMEM was removed and cells were incubated for 1 h in DMEM without FBS. Nanoparticles were incubated for 1 h for the protein corona formation. The cell incubation with the nanoparticles (75 µg mL^{-1}) was performed for 4 h at 37 °C and 5% CO$_2$ in DMEM without FBS. Afterward, cells were washed with PBS and detached from the cell culture plate using 0.25% Trypsin-EDTA. The viability staining was performed using Zombie Aqua (Biolegend) according to the manufacturer's manual. For the flow cytometry measurement cells were suspended in 1 mL PBS and 10 000 events recorded on Attune NxT Flow Cytometer. The BODIPY signal of nanoparticles was detected using the BL1 channel with an excitation laser of 488 nm and a 530/30 nm band pass filter and Zombie Aqua signal using VL2 channel with an excitation laser of 405 nm and a 512/25 nm band pass filter for emission. Data analysis was performed with Attune NxT Software selecting a cell population using a FSC/SSC scatter plot and excluding cell debris. Events were analyzed as percentage of gated events/cells and as median fluorescent intensity.

Confocal Laser Scanning Microscopy: In order to verify the intracellular localization of nanoparticles, the cLSM experiment was conducted using a Leica Laser Scanning Confocal Microscope (LSM SP5 STED Leica, Germany) equipped with a multi-laser combination and five detectors (range of 400–800 nm). Nanoparticles were detected using the 514 nm laser detecting at 530–600 nm. The cell membrane was stained shortly before measurement using 1:1000 dilution CellMaskDeepRed (5 mg mL^{-1} ThermoFisher Scientific), excited with the 633 nm laser and detected at 655–755 nm. Images were taken using LAS AF 3000 software and processed using Image J. For the confocal analysis, cells were seeded at a density of 50 000 cells per well in 8-well ibidi dishes and incubated overnight. The cell incubation with nanoparticles was performed in the same manner as in the flow cytometry experiment.

Analytical Tools: ^{1}H-NMR spectra were recorded on a Bruker Avance 250 spectrometer. Chemical shifts are denoted in ppm. Mass spectra were recorded with an Advion Expression L spectrometer. UV–vis and fluorescence spectra were recorded at room temperature on a Duetta absorbance and fluorescence spectrometer (Horiba). Fluorescence quantum yields were determined by the relative method using Lumogen Red (BASF) as reference.[32] The average size and the size distribution of the nanoparticles were measured by DLS at 25 and 37 °C using a Malvern Zetasizer Nano S90 (Malvern Instruments, UK) with a scattering angle of 90°. The samples were diluted with water to a concentration of ≈0.3 mg mL^{-1}. The zeta potential of the nanoparticles was measured with a Zeta Sizer Nano Series (Malvern Instruments, UK) at 25 °C. The nanoparticles were diluted with a 1 mM potassium chloride aqueous solution to a concentration of ≈0.5 mg mL^{-1}. The residual concentration of SDS in the dispersions was determined by using Stains-All assay.[33] The Stains-All was dissolved in isopropanol:water (1:1 v:v) at a concentration of 1 mg mL^{-1}. Thereafter, the Stains-All solution was mixed with 1 mL formamide and 18 mL water to prepare a working solution. A working solution without Stains-All was also prepared as a control. 1 µL of NPs dispersion was added to 200 µL working solution (or control solution). The absorbance was recorded at 438 nm by a Tecan INFINITE M1000 (Tecan Group Ltd., Switzerland). The measurements were performed in triplicate. The concentration of SDS (mg L^{-1}) was determined using a calibration curve for SDS prepared in the range of 0–721 mg L^{-1} water.

Supporting Information

Supporting Information is available from the Wiley Online Library or from the author.

Conflict of Interest

The authors declare no conflict of interest.

Data Availability Statement

The data that support the findings of this study are available from the corresponding author upon reasonable request.

[1] S. T. Yang, Y. Liu, Y. W. Wang, A. Cao, *Small* **2013**, *9*, 1635.

[2] T. L. Doane, C. Burda, *Chem. Soc. Rev.* **2012**, *41*, 2885.

[3] H. H. Gustafson, D. Holt-Casper, D. W. Grainger, H. Ghandehari, *Nano Today* **2015**, *10*, 487.

[4] P. C. Ke, S. Lin, W. J. Parak, T. P. Davis, F. Caruso, *ACS Nano* **2017**, *11*, 11773.

[5] S. Schöttler, G. Becker, S. Winzen, T. Steinbach, K. Mohr, K. Landfester, V. Mailänder, F. R. Wurm, *Nat. Nanotechnol.* **2016**, *11*, 372.

[6] V. H. Nguyen, B. J. Lee, *Int. J. Nanomed.* **2017**, *12*, 3137.

[7] J. Simon, T. Wolf, K. Klein, K. Landfester, F. R. Wurm, V. Mailänder, *Angew. Chem., Int. Ed.* **2018**, *57*, 5548.

[8] M. Mahmoudi, A. M. Abdelmonem, S. Behzadi, J. H. Clement, S. Dutz, M. R. Ejtehadi, R. Hartmann, K. Kantner, U. Linne, P. Maffre, S. Metzler, M. K. Moghadam, C. Pfeiffer, M. Rezaei, P. Ruiz-Lozano, V. Serpooshan, M. A. Shokrgozar, G. U. Nienhaus, W. J. Parak, *ACS Nano* **2013**, *7*, 6555.

[9] M. Mahmoudi, M. A. Shokrgozar, S. Behzadi, *Nanoscale* **2013**, *5*, 3240.

[10] C. Xue, N. Yonet-Tanyeri, N. Brouette, M. Sferrazza, P. V. Braun, D. E. Leckband, *Langmuir* **2011**, *27*, 8810.

[11] K. Nagase, M. Yamato, H. Kanazawa, T. Okano, *Biomaterials* **2018**, *153*, 27.

[12] A. Bordat, T. Boissenot, J. Nicolas, N. Tsapis, *Adv. Drug Delivery Rev.* **2019**, *138*, 167.

[13] J. Wang, E. Ayano, Y. Maitani, H. Kanazawa, *Int. J. Pharm.* **2017**, *523*, 217.

[14] K. Yoshimatsu, B. K. Lesel, Y. Yonamine, J. M. Beierle, Y. Hoshino, K. J. Shea, *Angew. Chem., Int. Ed.* **2012**, *51*, 2405.

[15] T. Cedervall, I. Lynch, M. Foy, T. Berggård, S. C. Donnelly, G. Cagney, S. Linse, K. A. Dawson, *Angew. Chem., Int. Ed.* **2007**, *46*, 5754.

[16] N. Bertrand, P. Grenier, M. Mahmoudi, E. M. Lima, E. A. Appel, F. Dormont, J. M. Lim, R. Karnik, R. Langer, O. C. Farokhzad, *Nat. Commun.* **2017**, *8*, 777.

[17] T. Bewersdorff, A. Gruber, M. Eravci, M. Dumbani, D. Klinger, A. Haase, *Int. J. Nanomed.* **2019**, *14*, 7861.

[18] Q. Yu, L. Zhao, C. Guo, B. Yan, G. Su, *Front. Bioeng. Biotechnol.* **2020**, *8*, 210.

[19] Y. Lu, M. Ballauff, *Prog. Polym. Sci.* **2011**, *36*, 767.

[20] F. J. Aangenendt, J. Mattsson, W. G. Ellenbroek, H. M. Wyss, *Phys. Rev. Appl.* **2017**, *8*, 014003.

[21] S. Winzen, J. C. Schwabacher, J. Müller, K. Landfester, K. Mohr, *Biomacromolecules* **2016**, *17*, 3845.

[22] K. Mohr, M. Sommer, G. Baier, S. Schöttler, P. Okwieka, S. Tenzer, K. Landfester, V. Mailänder, M. Schmidt, R. G. Meyer, *J. Nanomed. Nanotechnol.* **2014**, *5*, 1000193.

[23] Y. Hiruta, Y. Nagumo, Y. Suzuki, T. Funatsu, Y. Ishikawa, H. Kanazawa, *Colloids Surf. B* **2015**, *132*, 299.

[24] K. Rausch, A. Reuter, K. Fischer, M. Schmidt, *Biomacromolecules* **2010**, *11*, 2836.

[25] S. Jiang, D. Prozeller, J. Pereira, J. Simon, S. Han, S. Wirsching, M. Fichter, M. Mottola, I. Lieberwirth, S. Morsbach, V. Mailänder, S. Gehring, D. Crespy, K. Landfester, *Nanoscale* **2020**, *12*, 2626.

[26] S. Schöttler, K. Landfester, V. Mailänder, *Angew. Chem., Int. Ed.* **2016**, *55*, 8806.

[27] R. L. Johnson, K. Schmidt-Rohr, *J. Magn. Reson.* **2014**, *239*, 44.

[28] C. D. Thurmond, *J. Polym. Sci.* **1952**, *8*, 607.

[29] M. Kokkinopoulou, J. Simon, K. Landfester, V. Mailänder, I. Lieberwirth, *Nanoscale* **2017**, *9*, 8858.

[30] J. Simon, L. K. Müller, M. Kokkinopoulou, I. Lieberwirth, S. Morsbach, K. Landfester, V. Mailänder, *Nanoscale* **2018**, *10*, 10731.

[31] J. C. Silva, M. V. Gorenstein, G. Z. Li, J. P. Vissers, S. J. Geromanos, *Mol. Cell. Proteomics* **2006**, *5*, 144.

[32] A. M. Brouwer, *Pure Appl. Chem.* **2011**, *83*, 2213.

[33] F. Rusconi, E. Valton, R. Nguyen, E. Dufourc, *Anal. Biochem.* **2001**, *295*, 31.